Dynamic Multiphoton Microscopy: Focusing Light on Acute Kidney Injury

Andrew M. Hall[1] and Bruce A. Molitoris[2]

[1]Institute of Anatomy, University of Zurich, Zurich, Switzerland; and [2]Indiana University School of Medicine, Indiana Center for Biological Microscopy, Indianapolis, Indiana
andrew.hall@uzh.ch

Acute kidney injury (AKI) is a major global health problem; much research has been conducted on AKI, and numerous agents have shown benefit in animal studies, but none have translated into treatments. There is, therefore, a pressing unmet need to increase knowledge of the pathophysiology of AKI. Multiphoton microscopy (MPM) provides a tool to non-invasively visualize dynamic events in real time and at high resolution in rodent kidneys, and in this article we review its application to study novel mechanisms and treatments in different forms of AKI.

Acute kidney injury (AKI) is a major global health problem with significant associated morbidity and mortality (5, 36, 61). Common etiologies include ischemia-reperfusion injury (IRI), septic shock, drug toxicity, and glomerulonephritis (GN). Much research has been conducted on AKI in the last 50 years, and numerous putative therapeutic agents have shown benefit in animal studies, however, none of these have successfully translated into effective treatments for humans. There are, therefore, pressing unmet needs for further research in this field to increase knowledge of the pathophysiology of AKI at a cellular and subcellular level, identify new therapeutic targets, and understand the mechanisms of new therapeutic agents. Advanced live imaging techniques such as multiphoton microscopy (MPM) provide the potential to noninvasively visualize the aforementioned dynamic events in real time and at high resolution in rodent models of AKI.

In Vivo Kidney Imaging With Multiphoton Microscopy

Principles of Multiphoton Microscopy

Fluorescence microscopy is widely used to study physiological processes in cells in vitro; however, renal tubular cells tend to change their phenotype rapidly when removed from their native environment, which limits the usefulness of cell lines in translational research. Imaging of tubular cells in intact organs with standard confocal microscopy is possible (58), but this approach is constrained by the limited tissue penetration and significant photo-toxicity of visible wavelength lasers. MPM is a form of fluorescence imaging that utilizes a long wavelength laser, typically in the near infrared range (700–1,000 nm). The principle of MPM was first described in the 1930s, but it has only been used for biological imaging since the 1980s. Excitation of fluorescent molecules occurs due to the simultaneous arrival of two or more low-energy photons, and the probability of these events occurring is increased dramatically by pulsing the laser at very high frequency. In practical terms, most studies performed to date have used two-photon excitation; hence, the term "two-photon" microscopy rather than "multiphoton" is sometimes used in publications. MPM has several practical advantages for imaging intact organs (28, 31, 71). First, tissue penetration is increased due to decreased scattering of long-wavelength light. Second, lower excitation energy results in less tissue phototoxicity. Third, as the probability of excitation drops steeply away from the exact focal point of the laser, the level of out-of-plane signal is low, meaning that no pin-hole is required and all of the emitted light can be directly collected. Due to these distinct advantages, MPM has now become the gold standard approach for live imaging of cellular and subcellular processes in intact functioning organs and living animals, and is even being used to noninvasively evaluate skin lesions in humans (54).

Imaging the Kidney

MPM has now been used to image the rodent kidney for over a decade (for a comprehensive recent review, see Ref. 45), and it can be applied to both in vivo and in vitro preparations [including isolated glomeruli (46), tissue slices (27), and isolated perfused organs (25)]. Imaging the kidney in vivo requires the induction of adequate general anesthesia and exposure of the organ via a small flank incision in the abdomen (17). Both upright and inverted imaging approaches can be utilized; the former requires a cup to hold and support the kidney (similar to the setup for renal micro-puncture), and a glass cover slide is placed on top of the organ, and the microscope objective is lowered onto this. In the inverted approach, the animal is laid on the microscope stage, and the kidney is rested on a cover slide, below which the objective

is situated. The inverted approach typically leads to more stable conditions for acquiring images in the same focal plane over time due to dampening of movements caused by breathing and arterial pulsation. Maintenance of the health of the animal while under anesthesia is vital to maintain normal kidney function and obtain reliable and reproducible results. In particular, the temperature should be closely monitored and regulated with a stage heater or other appropriate device, and blood pressure should also be recorded. Monitoring of arterial pressure and a constant intravenous infusion of normal saline of Lactate Ringers ensures hydration and stable hemodynamics.

A range of extracellular and intracellular signals can be imaged in the kidney using MPM in animal models of AKI (42, 57). The tubular and vascular compartments can be visualized by using fluorescent molecules of different sizes that are either freely filtered or retained in the circulation, respectively. The rate of GFR can be calculated by measuring the decay of fluorescence signal emitted by the freely filtered molecules in the vasculature (69), and exploiting the same principle with fibreoptic ratiometric fluorescence analyzers may allow rapid point of care measurements in larger animals (68). Blood flow in the microvasculature can be assessed by measuring the velocity of red blood cells, and the movement and behavior of leukocytes can also be directly observed (56, 57). Label-free imaging techniques such as second harmonic generation can be used to visualize collagen deposition (60), a classic marker of tubulo-interstitial fibrosis. The high resolution of MPM allows detailed imaging of a range of intracellular structures in tubules, including cell nuclei, endosomes, lysosomes, renin granules, and mitochondria (26, 35, 51), whereas functional readouts such as mitochondrial energization, reactive oxygen species (ROS) production, glutathione levels, and Ca^{2+} signaling can also be acquired in real time (25, 26, 34, 44, 64).

Investigating Acute Kidney Injury With MPM

MPM has been used to investigate the pathogenesis of AKI and the effects of potential therapeutic interventions in a range of different rodent models, including IRI, sepsis, drug toxicity, and GN.

Ischemia-Reperfusion Injury

IRI is a common cause or contributing factor to AKI in both native and transplanted organs. It is typically studied in rodents by occluding the renal artery for 30–45 min with a clamp and then releasing it. This approach reliably causes AKI and is amenable to a live imaging approach; however, it remains debatable how transferable findings are to

humans where the etiology of AKI may be more complex (30). The effects of reduced, rather than absent, blood flow in the kidney can be investigated using partial occlusion of the aorta (56).

The main site of damage in IRI is the proximal tubule (PT) (55), which contains a high density of mitochondria but lacks anaerobic ATP-generating capacity and is thus exquisitely vulnerable to a disruption in oxygen supply (2). Mitochondrial NADH is the substrate for complex I in the respiratory chain and is naturally fluorescent only in the reduced state (11). We have shown that NADH can be imaged in tubular cells using MPM (FIGURE 1A) and provides a label-free readout of mitochondrial redox state (27). To investigate the effects of IRI on mitochondrial function in vivo, we devised a setup whereby the renal artery could be occluded remotely while imaging the kidney in real time. We found that occlusion of the renal artery caused an immediate and marked rise in the NADH signal in tubular cells, which then decreased again upon restoration of renal blood flow (26). These observations imply that mitochondria in tubular cells become hypoxic very rapidly upon cessation of renal blood flow, leading to decreased respiratory chain activity and pushing the NADH pool into a reduced state. They also support previous findings that mitochondrial substrates in the PT are in a relatively oxidized state under physiological conditions (13, 27, 37).

The normal activity of respiratory chain complexes within mitochondria generates a potential difference across the inner membrane ($\Delta\Psi_m$) that is central to mitochondrial function, determining processes such as ATP production and Ca^{2+} and protein import. Using established $\Delta\Psi_m$-dependent fluorescent dyes, which are rapidly taken up by tubular cells, we have previously shown that $\Delta\Psi_m$ decreases rapidly in the PT during ischemia, and is almost fully dissipated within minutes (25–27) (FIGURE 1, B AND C). The loss of $\Delta\Psi_m$ is associated with dramatic changes in mitochondrial morphology, such as swelling and fragmentation; visualization of these changes previously required electron microscopy of fixed specimens (7), but they can now be followed in real time using MPM (FIGURE 1D). During ischemia, $\Delta\Psi_m$ can be maintained to an extent by reverse activity of the ATP synthase (i.e., hydrolyzing ATP to maintain a proton gradient across the mitochondrial inner membrane), so long as there is a supply of ATP from anaerobic metabolism (10). Distal tubules (DTs) have significantly greater glycolytic capacity than PTs (2), and we found that both $\Delta\Psi_m$ and mitochondrial structure were better maintained in DTs during ischemia (FIGURE 1C) and that the maintenance of $\Delta\Psi_m$ was prevented by the ATP synthase inhibitor oligomycin (27). Taken together, our findings suggest that mitochondria in different nephron

segments respond differently to an ischemic insult, which may help to explain topographical patterns of damage in AKI.

The complex structure of the apical membrane of the PT is well adapted to perform large amounts of solute transport. It contains numerous microvilli to increase the surface area for reabsorption and a highly developed endocytotic apparatus to shuttle transporters to and from the membrane. The ar-

chitecture is supported by an extensive actin cytoskeleton that requires ATP to remain in a filamentous form (1). Using MPM, we have shown that ischemia and dissipation of $\Delta\Psi_m$ are associated with a rapid breakdown of the normal apical structure in PT cells within minutes, leading to dramatic membrane blebbing and extensive shedding of cytosolic contents and intact cells into the tubular lumen to form casts (FIGURE 1, E AND F) (25, 40). The striking speed and severity of these events suggest that the therapeutic time window in which they could be prevented is probably very short. Upon reperfusion, the intraluminal accumulation of cellular debris impedes tubular flow, helping to explain how a primary tubular insult such as IRI can cause a decrease in GFR during AKI.

Damage to microvascular endothelium in the kidney also occurs during IRI and causes sustained reductions in renal blood flow after the recommencement of perfusion (3, 63). Endothelial dysfunction and capillary dropout lead to hypoxia, which probably plays an important role in the development of tubulo-interstitial fibrosis and chronic kidney disease after an acute insult (4, 20). We have previously used MPM to investigate further the mechanisms of vascular loss during IRI (4). Using a transgenic mouse engineered to express YFP in endothelial cells and standard fluorescent markers of blood flow, it was shown that, following IRI, the YFP-positive cells in poorly perfused regions had enlarged and expanded into the surrounding interstitium and had taken on characteristics of fibroblasts. It is therefore likely that vascular dropout following IRI occurs at least in part due to phenotypic transition of endothelial cells.

IRI is a major contributor to delayed graft function in renal transplantation, as all grafts are exposed to at least a brief period of absent blood flow. Using an established surgical technique to transplant kidneys in mice, Camirand and coworkers were able to image the effects of IRI in grafts using MPM (9). Kidneys were transplanted en bloc using a long vascular pedicle, which allowed the organ to be maintained outside the recipient animal in an imaging cup, enabling direct access with a microscope objective. They acquired images for up to 3 h, following 15 and 25 min of cold and warm ischemia, respectively. Several pathological changes were noted in transplanted kidneys compared with native organs, including reduced filtration of low molecular weight dextrans, increased microvascular leakage, and greater numbers of apoptotic and necrotic tubular cells. In addition, abnormal movement of donor white blood cells was noted in the vasculature, including crawling along vessel walls. Interestingly, despite these significant functional abnormalities, only minimal damage was observed on light microscopy of fixed kidney specimens. The often striking disparity between functional and histological changes in AKI has been
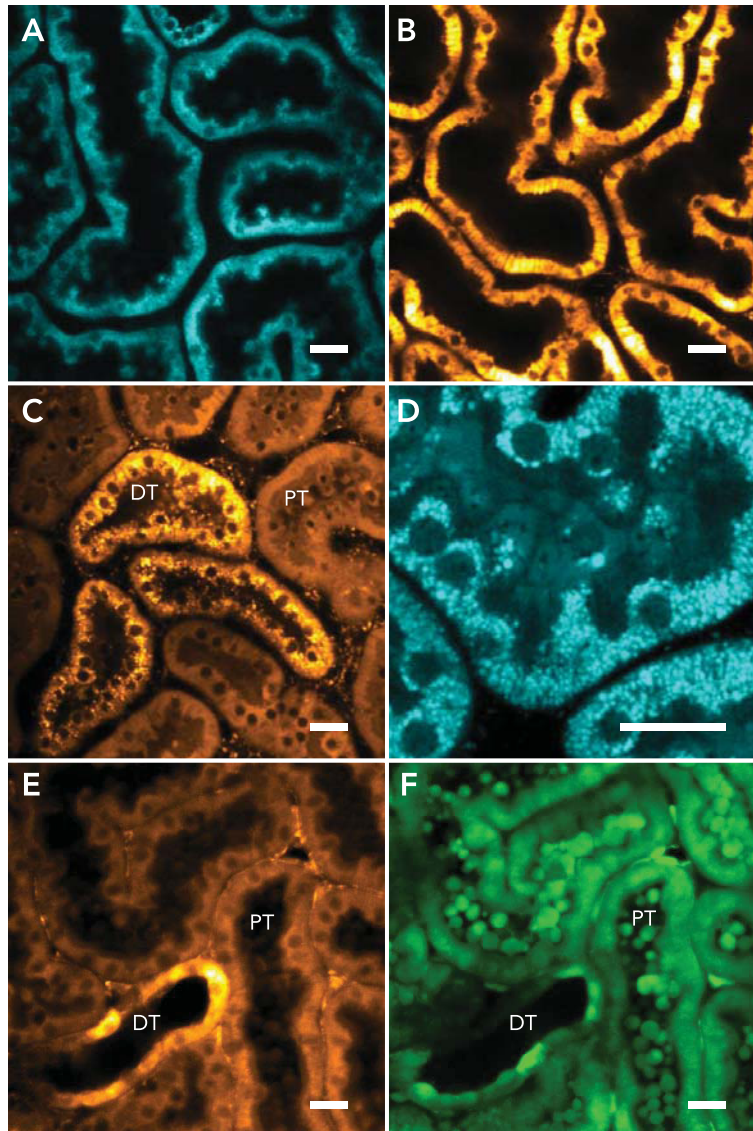
FIGURE 1. **Multiphoton imaging of mitochondrial structure and function in ischemic acute kidney injury**
A: mitochondrial NADH signal in rat proximal tubules (PTs) in vivo, showing a typical basolateral striated appearance. B: kidney tubules take up the mitochondrial membrane potential ($\Delta\Psi_m$)-dependent dye TMRM following an intravenous injection. C: during ischemia, $\Delta\Psi_m$ dissipates rapidly in PTs but is better maintained in distal tubules (DTs); the image depicted was acquired after 8 min of warm ischemia. D: depolarized mitochondria in the PT become swollen and fragmented during ischemia; the image depicted is of mitochondrial NADH and was acquired after 30 min of warm ischemia. E and F: tubular cells in an isolated perfused kidney co-loaded with TMRM and the cytosolic dye calcein green. After 10 min of warm ischemia, depolarization of mitochondria in PTs (E) is associated with extensive apical membrane blebbing and shedding of cellular debris into tubular lumens (F); in contrast, mitochondrial energization and cell structure are better maintained in DTs. Scale bars = 20 μm.

recognized for decades (49), and this further emphasizes the need for technologies such as live imaging.

Sepsis

Septicemia due to bacterial infection is a common cause of AKI, but the pathogenesis is poorly understood. Patients with septic shock often have a low blood pressure, which could cause renal ischemia, but this is not always the case, and AKI can occur in the absence of an overall reduction in renal blood flow (47). Hence, other important mechanisms may be occurring such as intrarenal blood shunting or direct impairment of tubular cell function, and MPM has been used in several studies to investigate the pathogenesis of septic AKI in rodent models.

Endotoxins such as lipopolysaccharides (LPS) are released by bacteria and can activate the host immune system, leading to a systemic immune response. Toll-like receptors (TLRs) are major receptors for microbial pathogens in the innate immune system and are expressed in the kidney (18). El-Achkar and coworkers showed that TLR4 is normally predominantly expressed in DTs in control rats, but after cecal ligation and puncture, a commonly used model of sepsis, there was a dramatic increase in expression in PTs (19). Following intravenous injection of fluorescent LPS, they noted rapid uptake at the PT brush border (within 10 min), and subsequent internalization into PT cells. More recently, it has been observed that endotoxin is taken up predominantly in the first (S1) segment of the PT and that this process is TLR4 dependent (34). Accumulation of endotoxin in S1 segments induced downstream oxidative stress (measured using ROS-sensitive fluorescent probes) in S2 regions, but surprisingly not in S1 segments themselves. The explanation(s) for this phenomenon remain unclear but could include higher expression of antioxidant defenses in the S1 segment or paracrine release of signaling molecules such as TNF-α from S1 cells that can induce oxidative stress in S2 cells (34). Taken together, these findings suggest that TLR4 plays an important role in mediating the renal response to sepsis and that rapid uptake of endotoxin occurs in the PT, which could directly cause tubular dysfunction independent of changes in renal blood flow.

Sepsis usually occurs secondary to overwhelming bacterial infections, and a common source of infection is the kidney itself (pyelonephritis). The most frequent cause of pyelonephritis is ascending infection from the lower urinary tract, a process that requires the firm attachment of bacteria to epithelial cells to prevent them being washed away in the urinary stream. Using real-time MPM and genetically engineered strains of pathogenic E. coli that express GFP, it has been shown that, when injected directly into nephrons, most bacteria are indeed washed away by luminal flow (38). However, sufficient numbers can still attach to epithelial cells, via fimbriae, to allow subsequent colonization of tubules, which then leads to obstruction of tubular flow and also induces thrombosis and occlusion of the microvasculature adjacent to the involved tubule. These events, along with hemodynamic changes caused by the systemic inflammatory response, help to explain how pyelonephritis can cause impairment of renal function.

Drug Toxicity

Another important etiological factor in the development of AKI during sepsis is the application of nephrotoxic drugs such as aminoglycoside antibiotics that are used to treat bacterial infections. The most frequently used agent in this class is gentamicin, which is a potent nephrotoxin. Gentamicin toxicity is specifically localized to the PT, and several previous in vitro studies have suggested that the drug causes impairment of mitochondrial function (50, 59, 72). We have recently investigated the tubular toxic effects of gentamicin in vivo using MPM of rats exposed to daily intraperitoneal injections of the drug (26), a model that reliably induces progressive renal failure over 7–10 days. We found that gentamicin caused rapid changes (within 1–2 days) in the structure of PTs, including enlargement of autofluorescent vesicles (most likely lysosomes) and abnormalities in the apical brush border. Subsequently, from 4 days onward, we observed changes in mitochondrial structure and function in PTs, with increased NADH signal and decreased $\Delta\Psi_m$ (FIGURE 2, A AND B). These changes were highly sporadic but became more widespread and severe over time, eventually leading to cell death by 7–8 days (FIGURE 2C). No abnormalities in mitochondrial signals were observed in DTs or collecting ducts. Taken together, these observations support the notion that gentamicin does cause mitochondrial dysfunction specifically in the PT but that there is significant spatial and temporal variability in the severity of effect, perhaps due to segmental differences in rates of endocytosis of the drug [the main uptake pathway (51)]. Furthermore, mitochondrial abnormalities occur secondary to earlier changes in other structures such as lysosomes, as suggested previously by in vitro studies (50).

Glomeluronephritis

Although less common than the above conditions, immune-mediated GN is also an important cause of AKI in humans, and MPM provides a method to investigate the behavior of immune cells in vivo (21). Various animal models of GN exist that mirror the human conditions and are potentially amenable to imaging experiments, but one drawback of working in the kidney is that depth of penetration

of infrared lasers in renal tissue is relatively poor (100–150 μm) compared with other organs such as the brain. This makes visualization of glomeruli difficult in rats; however, it is possible in mice and in certain strains of rat (Munich Wistar) that have more superficial glomeruli (FIGURE 3).

Another approach recently used to facilitate imaging of multiple glomeruli was to render mice hydronephrotic by prolonged ureteral ligation (15). In these experiments, fluorescent antibody-labeled neutrophils and GFP-expressing monocytes were noted to undergo periods of retention or crawling on capillary walls in glomeruli in control animals. Upon administration of anti-glomerular basement (anti-GBM) or anti-myeloperoxidase antibodies, which both cause aggressive renal failure in humans, the dwell times of circulating neutrophils and monocytes in glomeruli were significantly increased. This effect was specific to inflammatory GN, since it did not occur following puromycin aminonucleoside administration, which damages podocytes and causes nephrosis. Activated neutrophils produce H_2O_2 via NADPH oxidase, and the authors used a ROS-sensitive fluorescent dye to show that ROS production was increased in glomerular neutrophils in the GN models but not in NADPH oxidase-deficient mice. Integrins such as Mac-1 are transmembrane receptors that are thought to have important roles in leukocyte recruitment in vasculature, and the authors were able to show that inhibition of Mac-1 reduced ROS production in neutrophils and resulted in less glomerular damage (albuminuria). Taken together, these findings provide interesting new insights into the pathogenesis of GN and support the novel paradigm that circulating leukocytes normally interact with the vasculature in healthy glomeruli and that the development of GN principally involves increased retention and activation of these leukocytes, rather than an alteration in the number of new cells recruited to the kidney. However, some caution is necessary since the unilateral hydronephrotic obstruction (UUO) model is by itself a highly inflammatory model and is used by many investigators to study fibrosis.

Therapeutic Interventions

At present, treatment options for AKI remain limited, in particular in cases due to IRI or sepsis. Numerous experimental agents have shown efficacy in small animal studies but have not translated to human medicine (12). There are several potential explanations for this (24), but it is evident that there is a need for more sophisticated methods to evaluate the effects of potential treatments in more detail before moving to clinical trials. Several studies have now applied MPM to investigate putative therapies for AKI in vivo.

As discussed previously, regional alterations in renal blood flow contribute to the etiology and extension of AKI. Ischemia-induced endothelial dysfunction leads to inflammation, thrombosis, and occlusion of vessels, resulting in downstream tubular hypoxia and cell damage. Thrombomodulin is a glycoprotein expressed by endothelial cells that acts as a cofactor for the generation of activated protein C (APC), which is a potent anticoagulant and is protective in ischemic AKI in rats (39). Thrombomodulin is downregulated during ischemia, and this may contribute to a pro-thrombotic state. We showed in previous studies that subcutaneous administration of soluble thrombomodulin 24 h before renal IRI improved microvascular flow and reduced endothelial leukocyte rolling and attachment, and also lowered endothelial permeability (56). These improvements in endothelial function were associated with less tubular necrosis on histology and a reduction in renal impairment.
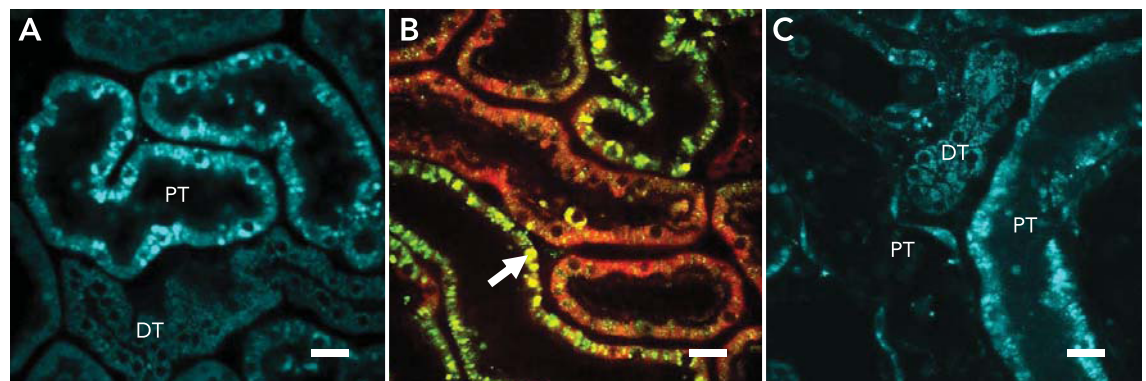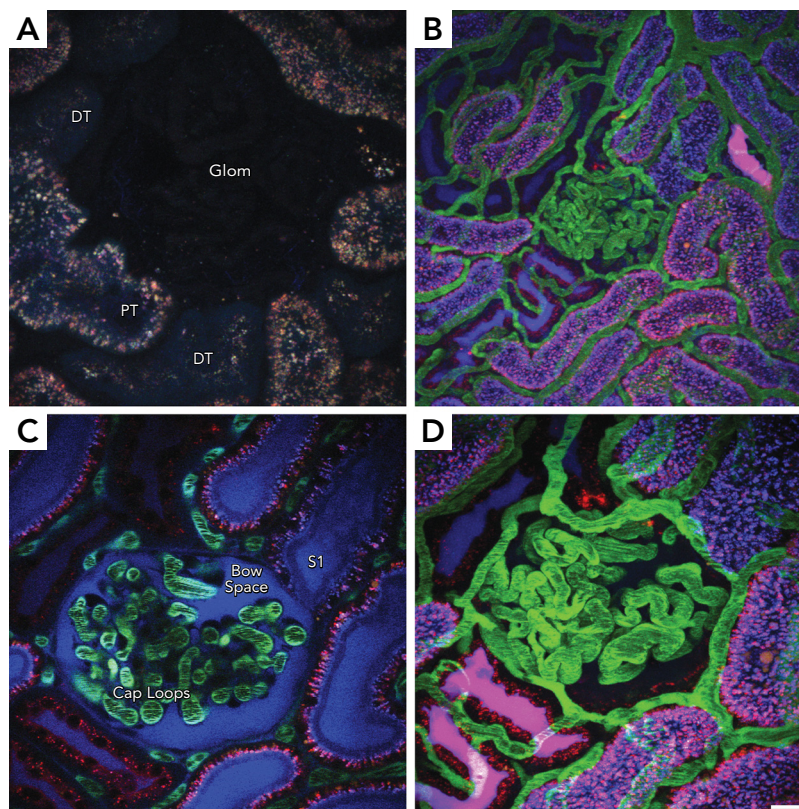

FIGURE 2. **In vivo multiphoton imaging of mitochondrial structure and function in gentamicin-induced acute kidney injury**
A: after 4 days of gentamicin administration, swollen mitochondria with increased NADH signal were observed in PTs but not in adjacent DTs. B: damaged PTs contained large green auto-fluorescent vesicles, probably representing enlarged lysosomes (arrow) and decreased TMRM signal (red), consistent with depolarized mitochondria. *C*: after 8 days, PTs showed severe damage with a highly irregular NADH signal, whereas DTs still retained a normal appearance; in the image depicted, the PT segment on the left is mostly devoid of living cells (a so-called ghost tubule). Scale bars = 20 μm.

APC has both antithrombotic and anti-inflammatory properties, and serum levels of APC decrease during sepsis. Administration of exogenous APC has been investigated as a clinical treatment for severe sepsis in humans, where it showed a beneficial effect on mortality but was associated with increased risk of bleeding (6). In a study using LPS-injected rats, in vivo MPM revealed that APC significantly improved capillary blood flow and reduced leukocyte adhesion, leading to reduced serum BUN levels, possibly via actions on inducible nitric oxide synthase and angiotensin II levels (22). These observations help to explain in more detail the previous findings in humans.

The PT avidly takes up small molecules from the surrounding environment via various transport processes such as receptor-mediated endocytosis. Although this is a disadvantage in one sense, since it predisposes the PT to accumulate circulating nephrotoxins, on the other hand this characteristic can be exploited therapeutically to target systemically injected protective agents to the PT (the major site of damage in most forms of AKI). Anti-sense oligonucleotides and small interfering RNA (siRNA) accumulate to very high levels in the kidney after systemic injection, and these molecules have attracted interest as tools to modulate intracellular stress responses in renal diseases. The tumor suppressor gene p53 plays a key role in regulating the cell cycle and can arrest growth or initiate apoptosis in response to cell stress (66). Increased p53 activity in the PT has been implicated in the pathogenesis of renal cell injury in AKI, and p53-deficient mice are protected in nephrotoxic models (70, 73); it therefore follows that inhibition of p53 activity might be an effective treatment strategy in AKI. Using in vivo MPM, we and others showed that fluorescently labeled siRNA is rapidly filtered and taken up by PT cells at the apical membrane following intravenous administration (41). Synthetic siRNA targeted to p53 was then injected both before and after IRI and was found to reduce p53 expression in the kidney, histological damage, and the number of apoptotic tubular cells. Protection was also seen in cisplatin-induced AKI, suggesting that the effects of p53 silencing are not limited to IRI. Following these promising initial results, in vivo MPM in a rat model of renal transplantation revealed that intravenous administration of siRNA to p53 improved microvascular blood flow, decreased the number of apoptotic/necrotic nuclei in tubular cells, and reduced intraluminal cast formation in the grafts (32). These changes were associated with improved kidney function, measured using serum creatinine.

Taken together, these previous studies suggest that silencing of p53 expression in the PT could be an effective treatment strategy in AKI due to IRI.

However, more recent experiments using p53-deficient mice have shown that paradoxically they actually experience greater renal dysfunction and fibrosis than wild-type animals following IRI (62). These conflicting results could perhaps be explained by species differences in the animal models used: in the rat, tubular cell apoptosis (probably activated by p53) is a major feature in IRI-induced AKI, and inhibition of p53 activity is thus protective. However, in the mouse, there is a major inflammatory response to ischemic injury, and the absence of p53 expression in leukocytes could lead to enhanced proliferation and activation (62).

FIGURE 3. **In vivo multiphoton imaging of surface glomeruli in Munich Wistar rats**
A: endogenous lysosomal auto-fluorescence in cell types in the kidney: PTs comprise most of the surface and are distinguished by their orange/brown fluorescence, whereas DTs appear darker with less autofluorescence. The glomerulus (Glom) is largely devoid of any autofluorescence, appearing as an empty circular space. *B*: a low-power micrograph of a three-dimensional volume shows the peritubular vasculature and glomerulus (*middle*) outlined with a large 150-kDa fluorescein dextran (green). Small 3-kDa dextrans labeled with either Texas Red (red) or Cascade Blue (blue) were introduced sequentially, filtered, and internalized by endocytosis in PTs (punctate accumulation); localization of these dextrans in the lumens of DTs appears as solid magenta or blue accumulations. *C*: single-plane image with a glomerulus in cross section (*middle*) with the capillary loops (Cap Loops) filtering out an additional bolus of the 3-kDa Cascade Blue dextran (blue) into the Bowman's space (Bow Space); the S1 segments is seen adjacent to the glomerulus. Red blood cells (RBCs) circulating within capillary loops and surrounding peritubular vessels appear as dark streaks from lack of dextran uptake. *D*: the PTs, seen in high power, show prominent accumulation of the two dextrans (appearing as punctate structures) within the endosomal pool; a DT (*bottom left*) is readily distinguished by the presence of the red and blue dextran in the lumen. A second DT (*top left*) is seen with a faint accumulation of the Cascade Blue dextran in the lumen. Scale bars = 20 μm in *A, C*, and *D*, and 40 μm in *B*.

These findings highlight the difficulties of translating experimental findings from a single animal species and reinforce the recognized need for realistic models of human AKI (30).

Current Challenges and Future Directions

The first decade or so of in vivo MPM in the kidney has generated many stunning images and has allowed fundamental physiological processes to be directly visualized for the first time. Furthermore, important scientific discoveries have been made relevant to AKI and other kidney diseases. However, MPM has not been without its drawbacks and controversies. New disruptive technologies inevitably generate novel and unexpected data that raise uncomfortable questions surrounding established "facts" and dogma in a field, leading to lively discussions and disagreements [a process emphatically illustrated by the recent debates over glomerular sieving coefficients (16, 52)]. So long as the limitations are clearly recognized and acknowledged, new research technologies will be the mechanisms behind paradigm shifts since they allow for new insights via unique avenues previously not available.

What exactly are the limitations for in vivo MPM in investigating AKI? First, the equipment required is expensive, although costs are coming down with time. Second, experimental animals are required, but this issue is not unique to imaging. Third, significant expertise is needed to surgically prepare and maintain the animals, maintain and optimize microscopes, and analyze and quantify acquired images using advanced computer software (pooling resources into a single core imaging facility is one solution to provide this broad range of skills). Fourth, as discussed above, with the typical tissue penetration of current lasers, imaging is limited to the outer cortex in the intact kidney, and glomeruli are difficult to visualize in most strains of rat. Finally, the loading of fluorescent probes into tubular cells in vivo in sufficient concentrations to make meaningful measurements of intracellular physiological processes also remains a technical challenge. Many commercially available dyes require long incubation times to accumulate into cells, and some of them are actively extruded by tubular cells, whereas AM-ester dyes can be cleaved by circulating esterases when injected into a live animal (33).

Nevertheless, despite these issues, MPM remains the gold standard approach to visualize and relate structure and function at cellular and subcellular levels in live animals, and the level of optical resolution intravitally achievable is unmatched by any other imaging technique. Furthermore, new technologies are emerging that could help to address some of the limitations of MPM. Increasing numbers of genetically modified mice are being generated that express fluorescent molecules in tissues of interest, and these have the potential to dramatically increase the scientific yield from in vivo MPM. For example, a very recent elegant study used mice expressing fluorescent markers in podocytes to track movement and migration of these cells within glomeruli over time, under both physiological and pathophysiological conditions, and revealed that the intraglomerular environment is much more dynamic than had previously been realized (23). Genetically encoded fluorescent sensors can also be introduced into tubular cells using micro-puncture (64, 65) or renal vein injection of plasmids or viral vectors (14). The depth of laser penetration achievable in the kidney will most likely be increased by the usage of new extended wavelength lasers (29, 67), and an expanding range of far-red excitation dyes, which emit in ranges where there is relatively little auto-fluorescence to mask their signals, are now commercially available. Also, new commercially available resonance scanning MPM, with enhanced PMT sensitivity, has increased the capture rate from 1 to ~30 full frames/s. Mice strains have recently been identified with superficial glomeruli amenable to high-resolution imaging (53), and the successful creation of abdominal imaging windows offers the potential to perform repeated imaging in the same animal over time (48) and thus follow the evolution of more chronic processes (e.g., recovery after AKI). Although not applicable to live imaging, organs harvested from mice can be "optically cleared" in vitro by replacing water in the tissues with a fluid with a similar refractive index to that of proteins, and this dramatically increases imaging depths to over 2 mm with MPM (43). Another recent technical development is the construction of multiphoton microendoscopes that allow minimally invasive imaging in vivo without the need to surgically externalize organs (8), and these could have clinical applications in humans.

To conclude, these are exciting times for in vivo MPM, which has proven to be a powerful tool in understanding the pathophysiology of AKI and in evaluating putative treatment strategies. It allows detailed real-time visualization of events at subcellular resolution in ways that were not previously possible. As such, MPM focuses light (both literally and metaphorically) on the fundamental dynamic processes that underlie AKI, which–sadly for many patients–have remained opaque for far too long. ∎

References

1. Atkinson SJ, Hosford MA, Molitoris BA. Mechanism of actin polymerization in cellular ATP depletion. *J Biol Chem* 279: 5194–5199, 2004.

2. Bagnasco S, Good D, Balaban R, Burg M. Lactate production in isolated segments of the rat nephron. *Am J Physiol Renal Fluid Electrolyte Physiol* 248: F522–F526, 1985.

3. Basile DP, Donohoe D, Roethe K, Osborn JL. Renal ischemic injury results in permanent damage to peritubular capillaries and influences long-term function. *Am J Physiol Renal Physiol* 281: F887–F899, 2001.

4. Basile DP, Friedrich JL, Spahic J, Knipe N, Mang H, Leonard EC, Changizi-Ashtiyani S, Bacallao RL, Molitoris BA, Sutton TA. Impaired endothelial proliferation and mesenchymal transition contribute to vascular rarefaction following acute kidney injury. *Am J Physiol Renal Physiol* 300: F721–F733, 2011.

5. Bellomo R, Kellum JA, Ronco C. Acute kidney injury. *Lancet* 380: 756–766, 2012.

6. Bernard GR, Vincent JL, Laterre PF, LaRosa SP, Dhainaut JF, Lopez-Rodriguez A, Steingrub JS, Garber GE, Helterbrand JD, Ely EW, Fisher CJ Jr. Efficacy and safety of recombinant human activated protein C for severe sepsis. *N Engl J Med* 344: 699–709, 2001.

7. Brooks C, Wei Q, Cho SG, Dong Z. Regulation of mitochondrial dynamics in acute kidney injury in cell culture and rodent models. *J Clin Invest* 119: 1275–1285, 2009.

8. Brown CM, Rivera DR, Pavlova I, Ouzounov DG, Williams WO, Mohanan S, Webb WW, Xu C. In vivo imaging of unstained tissues using a compact and flexible multiphoton microendoscope. *J Biomed Opt* 17: 040505, 2012.

9. Camirand G, Li Q, Demetris AJ, Watkins SC, Shlomchik WD, Rothstein DM, Lakkis FG. Multiphoton intravital microscopy of the transplanted mouse kidney. *Am J Transplant* 11: 2067–2074, 2011.

10. Campanella M, Parker N, Tan CH, Hall AM, Duchen MR. IF(1): setting the pace of the F(1)F(o)-ATP synthase. *Trends Biochem Sci* 34: 343–350, 2009.

11. Chance B, SCHOENERB, Oshino R, Itshak F, Nakase Y. Oxidation-reduction ratio studies of mitochondria in freeze-trapped samples. NADH and flavoprotein fluorescence signals. *J Biol Chem* 254: 4764–4771, 1979.

12. Chatterjee PK. Novel pharmacological approaches to the treatment of renal ischemia-reperfusion injury: a comprehensive review. *Naunyn Schmiedebergs Arch Pharmacol* 376: 1–43, 2007.

13. Coremans JM, Van AM, Naus DC, Van Velthuysen ML, Bruining HA, Puppels GJ. Pretransplantation assessment of renal viability with NADH fluorimetry. *Kidney Int* 57: 671–683, 2000.

14. Corridon PR, Rhodes GJ, Leonard EC, Basile DP, Gattone VH, Bacallao RL, Atkinson SJ. A method to facilitate and monitor expression of exogenous genes in the rat kidney using plasmid and viral vectors. *Am J Physiol Renal Physiol* 304: F1217–F1229, 2013.

15. Devi S, Li A, Westhorpe CL, Lo CY, Abeynaike LD, Snelgrove SL, Hall P, Ooi JD, Sobey CG, Kitching AR, Hickey MJ. Multiphoton imaging reveals a new leukocyte recruitment paradigm in the glomerulus. *Nat Med* 19: 107–112, 2013.

16. Dickson LE, Wagner MC, Sandoval RM, Molitoris BA. The proximal tubule and albuminuria: really. *J Am Soc Nephrol* 25: 443–453, 2014.

17. Dunn KW, Sandoval RM, Kelly KJ, Dagher PC, Tanner GA, Atkinson SJ, Bacallao RL, Molitoris BA. Functional studies of the kidney of living animals using multicolor two-photon microscopy. *Am J Physiol Cell Physiol* 283: C905–C916, 2002.

18. El-Achkar TM, Dagher PC. Renal Toll-like receptors: recent advances and implications for disease. *Nat Clin Pract Nephrol* 2: 568–581, 2006.

19. El-Achkar TM, Huang X, Plotkin Z, Sandoval RM, Rhodes GJ, Dagher PC. Sepsis induces changes in the expression and distribution of Toll-like receptor 4 in the rat kidney. *Am J Physiol Renal Physiol* 290: F1034–F1043, 2006.

20. Fine LG, Norman JT. Chronic hypoxia as a mechanism of progression of chronic kidney diseases: from hypothesis to novel therapeutics. *Kidney Int* 74: 867–872, 2008.

21. Germain RN, Robey EA, Cahalan MD. A decade of imaging cellular motility and interaction dynamics in the immune system. *Science* 336: 1676–1681, 2012.

22. Gupta A, Rhodes GJ, Berg DT, Gerlitz B, Molitoris BA, Grinnell BW. Activated protein C ameliorates LPS-induced acute kidney injury and downregulates renal INOS and angiotensin 2. *Am J Physiol Renal Physiol* 293: F245–F254, 2007.

23. Hackl MJ, Burford JL, Villanueva K, Lam L, Susztak K, Schermer B, Benzing T, Peti-Peterdi J. Tracking the fate of glomerular epithelial cells in vivo using serial multiphoton imaging in new mouse models with fluorescent lineage tags. *Nat Med* 19: 1661–1666, 2013.

24. Hall AM. Pores for thought: new strategies to re-energize stressed mitochondria in acute kidney injury. *J Am Soc Nephrol* 22: 986–989, 2011.

25. Hall AM, Crawford C, Unwin RJ, Duchen MR, Peppiatt-Wildman CM. Multiphoton imaging of the functioning kidney. *J Am Soc Nephrol* 22: 1297–1304, 2011.

26. Hall AM, Rhodes GJ, Sandoval RM, Corridon PR, Molitoris BA. In vivo multiphoton imaging of mitochondrial structure and function during acute kidney injury. *Kidney Int* 83: 72–83, 2013.

27. Hall AM, Unwin RJ, Parker N, Duchen MR. Multiphoton imaging reveals differences in mitochondrial function between nephron segments. *J Am Soc Nephrol* 20: 1293–1302, 2009.

28. Helmchen F, Denk W. Deep tissue two-photon microscopy. *Nat Methods* 2: 932–940, 2005.

29. Herz J, Siffrin V, Hauser AE, Brandt AU, Leuenberger T, Radbruch H, Zipp F, Niesner RA. Expanding two-photon intravital microscopy to the infrared by means of optical parametric oscillator. *Biophys J* 98: 715–723, 2010.

30. Heyman SN, Rosenberger C, Rosen S. Experimental ischemia-reperfusion: biases and myths-the proximal vs. distal hypoxic tubular injury debate revisited. *Kidney Int* 77: 9–16, 2010.

31. Hoover EE, Squier JA. Advances in multiphoton microscopy technology. *Nat Photonics* 7: 93–101, 2013.

32. Imamura R, Isaka Y, Sandoval RM, Ori A, Adamsky S, Feinstein E, Molitoris BA, Takahara S. Intravital two-photon microscopy assessment of renal protection efficacy of siRNA for p53 in experimental rat kidney transplantation models. *Cell Transplant* 19: 1659–1670, 2010.

33. Jobsis PD, Rothstein EC, Balaban RS. Limited utility of acetoxymethyl (AM)-based intracellular delivery systems, in vivo: interference by extracellular esterases. *J Microsc* 226: 74–81, 2007.

34. Kalakeche R, Hato T, Rhodes G, Dunn KW, El-Achkar TM, Plotkin Z, Sandoval RM, Dagher PC. Endotoxin uptake by S1 proximal tubular segment causes oxidative stress in the downstream S2 segment. *J Am Soc Nephrol* 22: 1505–1516, 2011.

35. Kang JJ, Toma I, Sipos A, Meer EJ, Vargas SL, Peti-Peterdi J. The collecting duct is the major source of prorenin in diabetes. *Hypertension* 51: 1597–1604, 2008.

36. Lameire NH, Bagga A, Cruz D, De MJ, Endre Z, Kellum JA, Liu KD, Mehta RL, Pannu N, Van BW, Vanholder R. Acute kidney injury: an increasing global concern. *Lancet* 382: 170–179, 2013.

37. Mayevsky A, Chance B. Oxidation-reduction states of NADH in vivo: from animals to clinical use. *Mitochondrion* 7: 330–339, 2007.

38. Melican K, Sandoval RM, Kader A, Josefsson L, Tanner GA, Molitoris BA, Richter-Dahlfors A. Uropathogenic *Escherichia coli* P and Type 1 fimbriae act in synergy in a living host to facilitate renal colonization leading to nephron obstruction. *PLoS Pathog* 7: e1001298, 2011.

39. Mizutani A, Okajima K, Uchiba M, Noguchi T. Activated protein C reduces ischemia/reperfusion-induced renal injury in rats by inhibiting leukocyte activation. *Blood* 95: 3781–3787, 2000.

40. Molitoris BA. Actin cytoskeleton in ischemic acute renal failure. *Kidney Int* 66: 871–883, 2004.

41. Molitoris BA, Dagher PC, Sandoval RM, Campos SB, Ashush H, Fridman E, Brafman A, Faerman A, Atkinson SJ, Thompson JD, Kalinski H, Skaliter R, Erlich S, Feinstein E. siRNA targeted to p53 attenuates ischemic and cisplatin-induced acute kidney injury. *J Am Soc Nephrol* 20: 1754–1764, 2009.

42. Molitoris BA, Sandoval RM. Multiphoton imaging techniques in acute kidney injury. *Contrib Nephrol* 165: 46–53, 2010.

43. Parra SG, Chia TH, Zinter JP, Levene MJ. Multiphoton microscopy of cleared mouse organs. *J Biomed Opt* 15: 036017, 2010.

44. Peppiatt-Wildman CM, Crawford C, Hall AM. Fluorescence imaging of intracellular calcium signals in intact kidney tissue. *Nephron Exp Nephrol* 121: e49–e58, 2012.

45. Peti-Peterdi J, Burford JL, Hackl MJ. The first decade of using multiphoton microscopy for high-power kidney imaging. *Am J Physiol Renal Physiol* 302: F227–F233, 2012.

46. Peti-Peterdi J, Fintha A, Fuson AL, Tousson A, Chow RH. Real-time imaging of renin release in vitro. *Am J Physiol Renal Physiol* 287: F329–F335, 2004.

47. Prowle J, Bagshaw SM, Bellomo R. Renal blood flow, fractional excretion of sodium and acute kidney injury: time for a new paradigm? *Curr Opin Crit Care* 18: 585–592, 2012.

48. Ritsma L, Steller EJ, Ellenbroek SI, Kranenburg O, Borel Rinkes IH, van RJ. Surgical implantation of an abdominal imaging window for intravital microscopy. *Nat Protoc* 8: 583–594, 2013.

49. Rosen S, Stillman IE. Acute tubular necrosis is a syndrome of physiologic and pathologic dissociation. *J Am Soc Nephrol* 19: 871–875, 2008.

50. Sandoval RM, Molitoris BA. Gentamicin traffics retrograde through the secretory pathway and is released in the cytosol via the endoplasmic reticulum. *Am J Physiol Renal Physiol* 286: F617–F624, 2004.

51. Sandoval RM, Molitoris BA. Quantifying endocytosis in vivo using intravital two-photon microscopy. *Methods Mol Biol* 440: 389–402, 2008.

52. Sandoval RM, Wagner MC, Patel M, Campos-Bilderback SB, Rhodes GJ, Wang E, Wean SE, Clendenon SS, Molitoris BA. Multiple factors influence glomerular albumin permeability in rats. *J Am Soc Nephrol* 23: 447–457, 2012.

53. Schiessl IM, Bardehle S, Castrop H. Superficial nephrons in BALB/c and C57BL/6 mice facilitate in vivo multiphoton microscopy of the kidney. *PLos One* 8: e52499, 2013.

54. Seidenari S, Arginelli F, Bassoli S, Cautela J, French PM, Guanti M, Guardoli D, Konig K, Talbot C, Dunsby C. Multiphoton laser microscopy and fluorescence lifetime imaging for the evaluation of the skin. *Dermatol Res Pract* 2012: 810749, 2012.

55. Shanley PF, Rosen MD, Brezis M, Silva P, Epstein FH, Rosen S. Topography of focal proximal tubular necrosis after ischemia with reflow in the rat kidney. *Am J Pathol* 122: 462–468, 1986.

56. Sharfuddin AA, Sandoval RM, Berg DT, McDougal GE, Campos SB, Phillips CL, Jones BE, Gupta A, Grinnell BW, Molitoris BA. Soluble thrombomodulin protects ischemic kidneys. *J Am Soc Nephrol* 20: 524–534, 2009.

57. Sharfuddin AA, Sandoval RM, Molitoris BA. Imaging techniques in acute kidney injury. *Nephron Clin Pract* 109: 198–204, 2008.

58. Simeoni M, Boyde A, Shirley DG, Capasso G, Unwin RJ. Application of red laser video-rate scanning confocal microscopy to in vivo assessment of tubular function in the rat: selective action of diuretics on tubular diameter. *Exp Physiol* 89: 181–185, 2004.

59. Simmons CF Jr, Bogusky RT, Humes HD. Inhibitory effects of gentamicin on renal mitochondrial oxidative phosphorylation. *J Pharmacol Exp Ther* 214: 709–715, 1980.

60. Strupler M, Hernest M, Fligny C, Martin JL, Tharaux PL, Schanne-Klein MC. Second harmonic microscopy to quantify renal interstitial fibrosis and arterial remodeling. *J Biomed Opt* 13: 054041, 2008.

61. Susantitaphong P, Cruz DN, Cerda J, Abulfaraj M, Alqahtani F, Koulouridis I, Jaber BL. World incidence of AKI: a meta-analysis. *Clin J Am Soc Nephrol* 8: 1482–1493, 2013.

62. Sutton TA, Hato T, Mai E, Yoshimoto M, Kuehl S, Anderson M, Mang H, Plotkin Z, Chan RJ, Dagher PC. p53 is renoprotective after ischemic kidney injury by reducing inflammation. *J Am Soc Nephrol* 24: 113–124, 2013.

63. Sutton TA, Mang HE, Campos SB, Sandoval RM, Yoder MC, Molitoris BA. Injury of the renal microvascular endothelium alters barrier function after ischemia. *Am J Physiol Renal Physiol* 285: F191–F198, 2003.

64. Svenningsen P, Burford JL, Peti-Peterdi J. ATP releasing connexin 30 hemichannels mediate flow-induced calcium signaling in the collecting duct. *Front Physiol* 4: 292, 2013.

65. Tanner GA, Sandoval RM, Molitoris BA, Bamburg JR, Ashworth SL. Micropuncture gene delivery and intravital two-photon visualization of protein expression in rat kidney. *Am J Physiol Renal Physiol* 289: F638–F643, 2005.

66. Vousden KH, Prives C. Blinded by the light: the growing complexity of p53. *Cell* 137: 413–431, 2009.

67. Wang C, Qiao L, He F, Cheng Y, Xu Z. Extension of imaging depth in two-photon fluorescence microscopy using a long-wavelength high-pulse-energy femtosecond laser source. *J Microsc* 243: 179–183, 2011.

68. Wang E, Meier DJ, Sandoval RM, Von Hendy-Willson VE, Pressler BM, Bunch RM, Alloosh M, Sturek MS, Schwartz GJ, Molitoris BA. A portable fiberoptic ratiometric fluorescence analyzer provides rapid point-of-care determination of glomerular filtration rate in large animals. *Kidney Int* 81: 112–117, 2012.

69. Wang E, Sandoval RM, Campos SB, Molitoris BA. Rapid diagnosis and quantification of acute kidney injury using fluorescent ratio-metric determination of glomerular filtration rate in the rat. *Am J Physiol Renal Physiol* 299: F1048–F1055, 2010.

70. Wei Q, Dong G, Yang T, Megyesi J, Price PM, Dong Z. Activation of p53 in cisplatin-induced nephrotoxicity. *Am J Physiol Renal Physiol* 293: F1282–F1291, 2007.

71. Weigert R, Porat-Shliom N, Amornphimoltham P. Imaging cell biology in live animals: ready for prime time. *J Cell Biol* 201: 969–979, 2013.

72. Weinberg JM, Simmons F Jr, Humes HD. Alterations of mitochondrial respiration induced by aminoglycoside antibiotics. *Res Commun Chem Pathol Pharmacol* 27: 521–531, 1980.

73. Zhou L, Fu P, Huang XR, Liu F, Lai KN, Lan HY. Activation of p53 promotes renal injury in acute aristolochic acid nephropathy. *J Am Soc Nephrol* 21: 31–41, 2010.